HIGH SCHOOL EDITION
Journal of Student Research
Volume 12 Issue 3 (2023)

Identifying Locations for Transcranial Magnetic Stimulation Coil Placement for Deep Brain Structures

Tanush Paradeshi[1] and Mimi Liljeholm[#]

[1]University High School, USA
[#]Advisor

ABSTRACT

Stimulation of deep brain structures with transcranial magnetic stimulation (TMS) is the premier mode of non-invasive brain stimulation (NIBS). Currently, there is little support for the application of TMS in modulating deeper brain structures. This study validates the use of TMS for a set of 8 deep brain structures shown to alleviate symptoms of certain conditions when stimulated. 200 sets of T1-weighted and T2-weighted MRIs were processed using the SimNIBS headreco pipeline. Then, 200 TMS optimization simulations were run for each brain structure, which generated 200 3D coordinates for each structure representing the best TMS coil placement locations on the scalp for stimulation. This data was analyzed using K-means and agglomerative clustering methods to find the overall best coil placement locations. Overall, this study validates the use of TMS to stimulate these brain structures and finds the optimal parameters for stimulation.

Introduction

According to the UN, nearly 1 in 6 individuals globally suffer from neurological conditions. Conventional treatments for neurological conditions including therapy and medication are expensive and often ineffective for a significant portion of patients. Thus, alternative techniques for treatments have been developed, including neurostimulation techniques which serve to modulate nervous system activity within the body to alleviate or perhaps even cure certain conditions. These technologies include deep brain stimulation (DBS), transcranial magnetic stimulation (TMS), transcranial direct current stimulation (tDCS) and transcranial alternating current stimulation (tACS) among other stimulation techniques. However, there is currently a lack of consensus regarding how these technologies can be used safely and effectively, especially regarding TMS, tDCS and tACS as these are all relatively new technologies. Moreover, with recent advances in simulation techniques, the potential of these technologies are rapidly growing and it is thus imperative to characterize their usage.

Background

The research is specifically focused on transcranial magnetic stimulation (TMS), a recently introduced neurotechnology capable of altering neural activity in superficial areas of the brain. TMS is completely non-invasive and involves the placement of a removable coil structure on a patient's scalp from which magnetic waves are emitted. This coil is placed during TMS stimulation sessions which usually occur a few times a week with duration and stimulation intensity varying on a patient-to-patient basis. This technology is currently being used to treat conditions including Obsessive Compulsive Disorder (OCD) and Major Depression. Whether this technology is able to help treat other conditions is currently being investigated. As an alternative to TMS, Deep

Brain Stimulation (DBS) is the gold-standard stimulation technique involving the placement of electrode(s) into specific target regions of the brain. These electrodes produce electric impulses which can modulate brain activity. DBS has been FDA-approved to treat a variety of conditions including Parkinson's, epilepsy, essential tremor, dystonia, and OCD.

Additionally, current clinical trials show promising results in the application of DBS for Depression, bipolar disorder, chronic pain and PTSD among other conditions. However, DBS implantation is an invasive procedure as it involves drilling small holes in the skull and directly implanting electrodes within brain tissue. A small device containing batteries must also be implanted (usually in the chest region) to power the implanted electrodes. Such a procedure raises many risks including bleeding, stroke, infection, breathing problems, nausea, heart problems and seizure. Additionally, DBS is ineffective in some patients, especially for treating conditions that DBS has not received FDA-approval for. Moreover, DBS usually incurs costs around $35,000 $50,000 while often exceeding $100,000 in bilateral procedures (with electrodes being implanted on both sides of the brain). Finally, the surgical procedure associated with DBS is often not compatible for many patients such as the elderly, individuals at greater risk for complications or with other pre-existing neurological conditions. In contrast, TMS is completely non-invasive and significantly less expensive as it usually involves costs of $300 per session, with full treatments usually costing between $6,000 and $12,000. Thus, TMS is generally more accessible and has the potential to become the preferred mode of treatment.

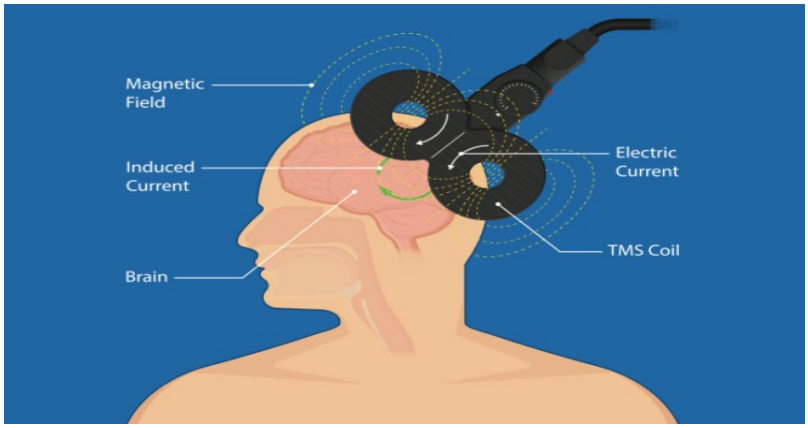

Figure 1. Coil induced magnetic waves modulate superficial cortical networks. http://sapienlabs.org/the-basics-of-transcranial-magnetic-stimulation

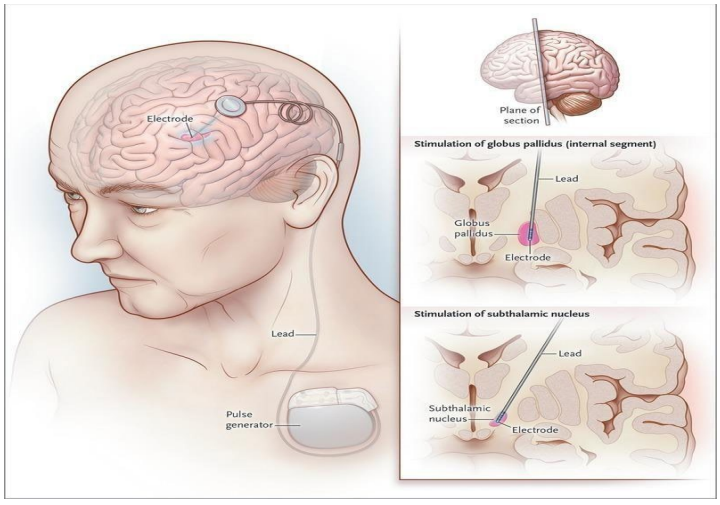

Figure 2. DBS components including electrodes with battery in chest region implanted through invasive surgery. https://www.nejm.org/doi/full/10.1056/NEJMct1208070

However, since TMS involves emitting magnetic waves from an external coil, it is most effective at modulating superficial brain activity. Wave intensity drops drastically when passing through tissue, rendering TMS unable to penetrate into deeper neural circuits. Thus, deep TMS coils such as the H1 coil and double-cone coil have been developed which are geometrically and structurally optimized at minimizing the rate of wave dissipation. There have also been studies validating the effectiveness of these TMS coils in stimulating various deep brain structures implicated in disease. Nevertheless, there has still been minimal work done in this area and how it is possible to achieve the best results when targeting deeper brain structures is largely unknown. Thus, this study aims to discover the best coil position for optimal stimulation. Such a study would greatly advance the study of non-invasive brain stimulation techniques as well as mathematically validate the use of TMS for a variety of other conditions based on modeling and simulations.

Methods

This research focused on eight target brain structures which are each implicated in certain neurological diseases: subthalamic nucleus (for Parkinson's disease), amygdala (for epilepsy and PTSD), periaqueductal gray matter (for chronic pain), fornix (for Alzheimer's disease), ventrointeromedial nucleus of the thalamus (for tremor associated with multiple sclerosis and epilepsy), hippocampus (for epilepsy and PTSD), globus pallidus internus (for Parkinson's disease) and anterior cingulate cortex (for chronic pain). These structures were derived from a literature search on *PubMed* and each of these structures has been shown to alleviate symptoms of their associated conditions if stimulated. Thus, this research focuses on deriving the optimal coordinates for coil placement to achieve optimal stimulation of these structures. The H1 TMS coil was used in all simulations as it is the most common deep TMS coil with mechanical properties allowing for the magnetic field emitted to dissipate less rapidly as it penetrates brain tissue, making it optimal for types of TMS stimulation. These properties are derived from the tangential orientation of coil elements in reference to the scalp surface while non-tangential coil elements are minimized. The H1 coil also contains a flexible base, allowing for maximal magnetic coupling when attached to the scalp. The simulations were done using SimNIBS, the premier software for non-invasive brain stimulation simulations.

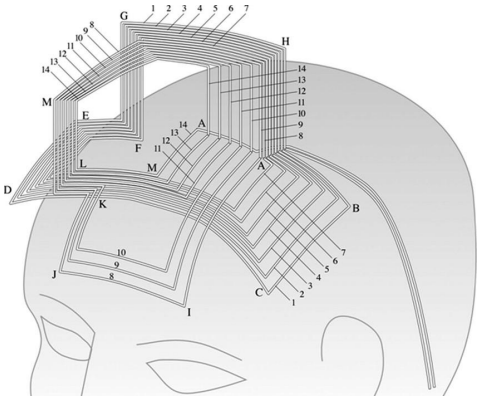

Figure 3. H1 coil flexible base placed om patient with non-tangential coil elements minimized. https://www.researchgate.net/figure/sketch-of-the-H1-coil-Hesed-near-a-human-head-The-coil-position-and-orientation_fig6_6526365

To conduct this research, T1-weighted and T2-weighted MRI files were retrieved from the IXI Dataset, a part of the Neuroimaging Tools and Resources Collaboratory website. The data set was public, and files were strictly confidential with no identifiable information associated with any files. 200 T1-weighted and 200 corresponding T2-weighted MRI files from the same set of patients were retrieved from the dataset. These files were reconstructed into a format suitable for running simulations through the headreco pipeline of SimNIBS. The pipeline involved the segmentation of major tissues (gray matter, white matter, cerebrospinal fluid, skull and scalp). A volume conductor model was also created in this process, which is used in simulations. This reconstruction process integrates input of a corresponding pair of T1-weighted and T2-weighted MRIs from the same patient and generates a mesh file for visualization of the reconstruction result as well as a folder of NifTI files corresponding to segmented portions of the MRI scans. T2-weighted MRIs were included in this process in conjunction with T1-weighted MRIs as it facilitates increased accuracy of segmentation on the border between the skull and cerebrospinal fluid (CSF). This is particularly crucial as the skull has a low electrical conductivity whereas CSF is conducting, which can thus largely affect simulation results. These segmentations were done using SPM12 and CAT12 software (included in headreco pipeline), which create surface reconstructions of gray matter. Finally, a finite element mesh is created by filling tetrahedrons between tissue surfaces. After segmentation of these processes occurred, the mesh files were visualized using MATLAB and the neuroimaging software package FreeSurfer to verify segmentation was done accurately. 200 headreco processes were scripted, each corresponding to a pair of T1-weighted and T2-weighted MRI scans from the same patient with each process computing for approximately 3-4 hours.

TMS simulations were then run using the SimNIBS software in which 200 simulations were performed for each brain structure, each simulation corresponding to one mesh file from the headreco processes. Each mesh file was simulated 8 times, corresponding to the 8 selected brain structures. Thus, overall, 1600 simulations were scripted, each corresponding to one brain structure and one mesh file. Coordinate input parameters corresponding to where the brain structure is located in the mesh file was provided for each simulation. In return, SimNIBS TMS simulations iteratively simulates sites across a patient's scalp to determine the location of the optimal coil placement for stimulation of the coordinates specified as input (corresponding to a brain structure). Simulations occur through the calculation of magnetic vector potentials for the coil model, position and current in question. The simulation is solved using finite element analysis with linear basis functions. This system is solved through an interactive preconditioned conjugate gradient method. Each simulation was run for approximately 1-2 hours and thus 2 virtual PaperSpace machines were used in conjunction with a local machine to perform these simulations. Coordinates of the selected brain structures were first converted into the Montreal Neurological Institute (MNI) space before providing the coordinates as input to TMS simulations. This is essential as subject coordinates corresponding to each brain structure vary across different MRI scans. Such variations in coordinate locations results in the inability to directly compare coordinates. In contrast, all coordinates in the MNI space are centralized such that any point corresponding to an anatomical location has only one coordinate in the MNI space, regardless of the coordinate of it in the specifi MRI scan from which it was taken. Transformations into MNI space involve the use of affine transformation matrices which contain specific information regarding the transformations required to shift between MNI and subject space for the particular MRI it is associated with. Specifically, the matrices specify linear transformations of translations, zooms and rotations needed to shift to and from MNI space.

```
Best coil position
============================
[[ -0.1743512   -0.47757441   0.86111807 -80.44158926]
 [ -0.86155917   0.49742142   0.10142844   2.41238018]
 [ -0.4767782   -0.72422     -0.49818464 -64.52103762]
 [  0.           0.           0.           1.        ]]
```

Figure 4. Sample Affine Transformation Matrix

Data Analysis and Results

After the best coordinate locations for stimulating target structures were collected, unsupervised machine learning algorithms were employed to analyze the coordinates for each brain structure. Agglomerative clustering and K-means clustering methods were used to find and analyze trends in the 3D coordinates. The TMS simulations returned a set of 3D coordinates corresponding to the best locations for coil placement. Thus, 200 3D coordinates were obtained for each of the 8 selected brain structures since 200 simulations were performed for each brain structure. The 200 3D coordinates for each brain structure were analyzed separately from all other brain structures. By clustering the coordinates for each brain structure, it's possible to identify regions on the scalp corresponding to the 3D coordinates located within each cluster that are optimal for placement of the TMS coils. For example, if 2 clusters are formed for a brain structure, the centers (average of all the coordinates within the cluster) of the clusters would represent the overall 2 best locations for placement of the TMS coil for stimulation of that brain structure.

First, KMeans clustering was used on the 200 coordinates for each brain structure. The elbow method was used to determine the number of clusters to select as it is one of the most popularly used methods to do so. Specifically, an inertia vs number of clusters graph is generated in which inertia is a measure of how well the dataset has been clustered by KMeans. Specifically, inertia is the sum of the squared distances between each data point and the center of the cluster it is in. Since it is desirable for inertia to be low and number of clusters to be low, the point at which the inertia started to decrease at a negligible amount as the number of clusters increased was selected. This resulted in 3 clusters being selected to perform KMeans clustering on the 200 coordinates for the subthalamic nucleus, 2 clusters for the hippocampus, 2 clusters for the amygdala, 2 clusters for the globus pallidus, 2 clusters for the anterior cingulate cortex, 2 clusters for the periaqueductal gray, 3 clusters for the fornix and 2 clusters for the ventrointeromedial nucleus of the thalamus. Having the number of clusters to use for each brain structure, clustering was then performed on the 200 coordinates for each brain structure, and the coordinates of the centroids (centers of the clusters) was computed as follows:

	Subthalamic	Hippocampus	Amygdala	Globus Pallidus	ACC	Perigray	Fornix	Venintmednuc
Cluster 1	-85.98, -12.93, -14.72	-85.31, -23.14, -9.10	-83.83, -0.31, -9.14	-84.31, -7.58, -22.25	-33.28, 43.16, 70.35	46.67, -36.45, -59.57	38.99, 10.01, 80.47	-84.99, -8.65, -1.68

Cluster 2	-78.43, 0.31, -35.94	-78.88, -30.45, -58.37	-77.29, -21.99, -58.88	-85.39, -8.02, 3.50	-77.54, -101.558, -107.029	-80.96, -31.14, -36.96	-43.29, 11.08, 80.86	-64.60, 6.56, 60.08
Cluster 3	-82.65, -0.17, 15.20						-70.74, 12.97, 46.81	

The number of centroids there are for each brain structure is equal to the number of clusters there are for each brain structure because the centroids represent the centers of each cluster. These centroids are essentially the multi-dimensional average of the 3D coordinates within each cluster. The coordinates of the centroids can thus be designated as the optimal locations for coil placement that have been determined by averaging the 200 optimal 3D coordinates, which were specific to each of the 200 patients used in the IXI dataset. To visualize the results of K-Means clustering, the 3D coordinates were compressed to 2D coordinates using Principal Component Analysis, a dimensionality reduction technique that preserves as much variability in the data as possible. After reducing the dimensionality of the data, K-means clustering was then performed and the results were plotted. Below is the result of performing dimensionality reduction and KMeans clustering on the 200 3D coordinates for the amygdala structure:

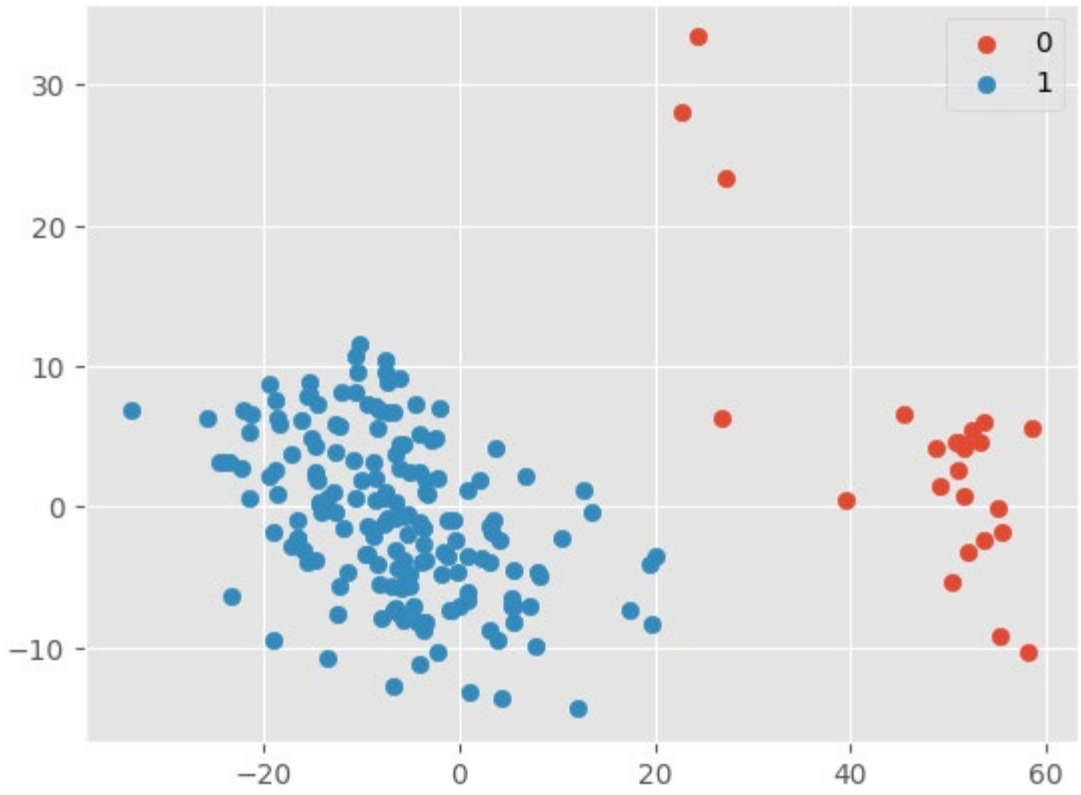

Agglomerative clustering methods were also used to identify trends in the data. Each data point is initially treated as an individual cluster and pairs of clusters are merged until all the data points have merged into a single cluster. This merging process can be visualized using a dendrogram as shown below:

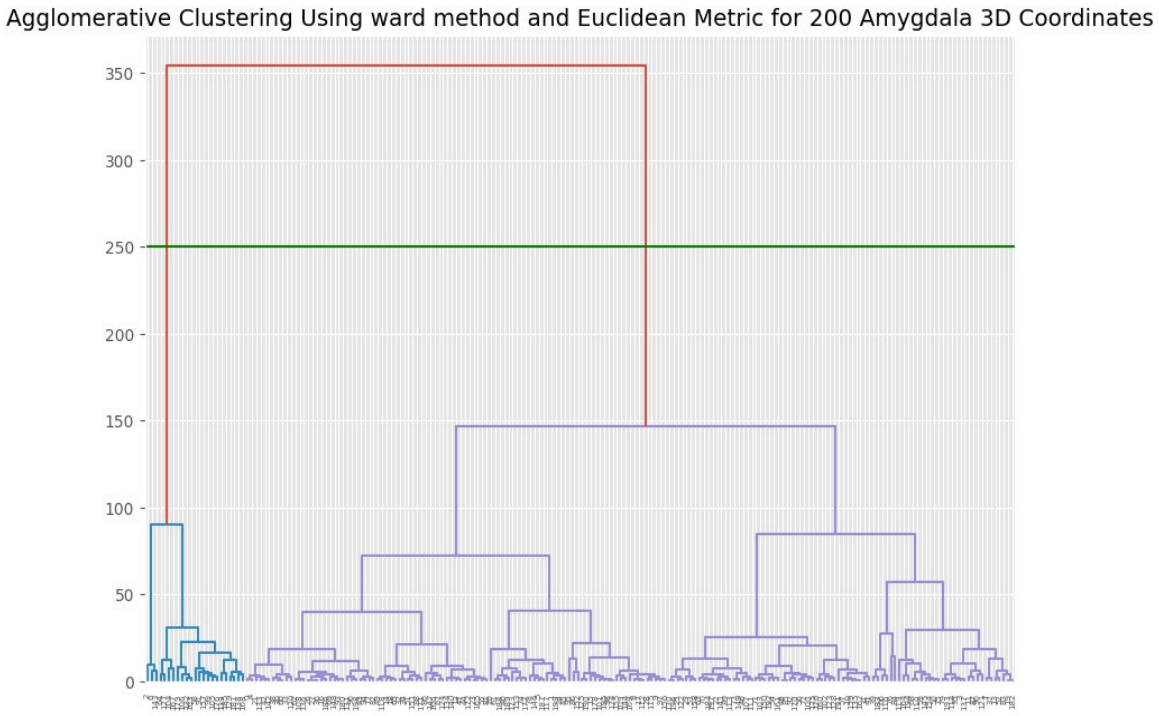

Different metrics (methods of calculating distances between data points) and methods (procedures for merging clusters) can be used to generate different results. The number of clusters to choose can be deduced by considering the largest vertical merge (red in the above dendrogram) and checking how many times a horizontal line intersects vertical lines at the level of that largest vertical merge (2 intersections in the above dendrogram indicating 2 clusters). The average of the data points in the clusters can then be computed (analogous to centroids in KMeans Clustering). The following table shows the coordinates of the average of the data points in the clusters using ward method and Euclidean metric:

	Subthalamic	Hippocampus	Amygdala	Globus Pallidus	ACC	Perigray	Fornix	Venintmednuc
Cluster 1	-82.77, -6.87, -24.87	-85.33, -23.35, -10.22	-83.80, -0.48, -9.56	-85.82, -15.70, -21.30	-19.77, 46.63, 76.45	-80.96, -31.14, -36.96	-54.39, 12.01, 68.14	-66.42, 3.30, 57.32
Cluster 2	-84.06, -5.49, 9.31	-78.78, -30.47, -58.65	-76.99, -22.53, -59.98	-85.77, -9.51, 3.61	-77.54, -101.56, -107.03	46.67, -36.45, -59.57	26.65, 9.32, 83.89	-85.06, -7.29, -3.94
Cluster 3				-78.64, 21.22, -21.05	-45.13, 40.12, 65.00			

The following table shows the average of the data points in the clusters using complete method and chebyshev metric:

	Subthalamic	Hippocampus	Amygdala	Globus Pallidus	ACC	Perigray	Fornix	Venintmednuc
Cluster 1	-83.35, -7.64, -21.11	-85.34, -23.20, -9.63	-77.29, -22.00, -58.88	-84.97, -7.36, -6.94	-33.28, 43.16, 70.35	-80.96, -31.14, -36.96	-51.49, 11.91, 70.11	-84.10, -4.98, 1.01
Cluster 2	-82.87, -2.09, 16.78	-78.82, -30.48, -58.52	-83.83, -0.31, -9.14	-77.5, -102.0, -107.0	-77.54, -101.56, -107.03	46.67, -36.45, -59.57	41.10, 8.84, 79.82	-63.94, 1.36, 62.14

Similarities between the averages of the data points in each cluster in both versions of agglomerative clustering and centroids in K-means suggests there are a few general optimal areas on the scalp for placement of TMS coils for stimulation of these 8 different brain structures.

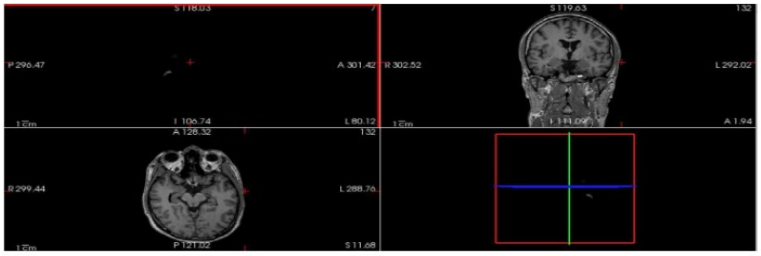

Fig 8. Optimal Coil Placement location for stimulation of subthalamic nucleus as indicated by the cross in top right and bottom left windows

Fig 9. Optimal Coil Placement location for stimulation of amygdala as indicated by the cross in top right and bottom left windows

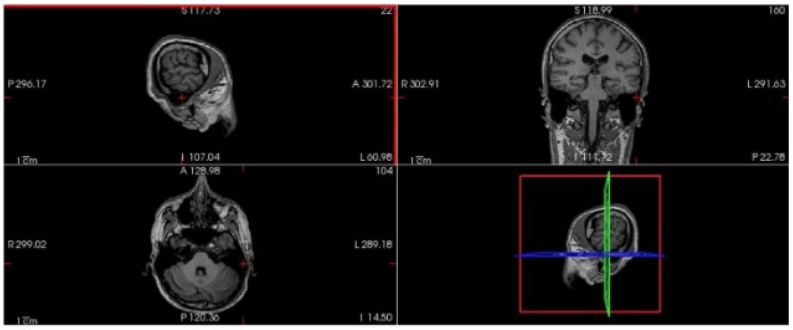

Fig 10. Optimal Coil Placement location for stimulation of periaqueductal gray matter as indicated by the cross in top right and bottom left windows

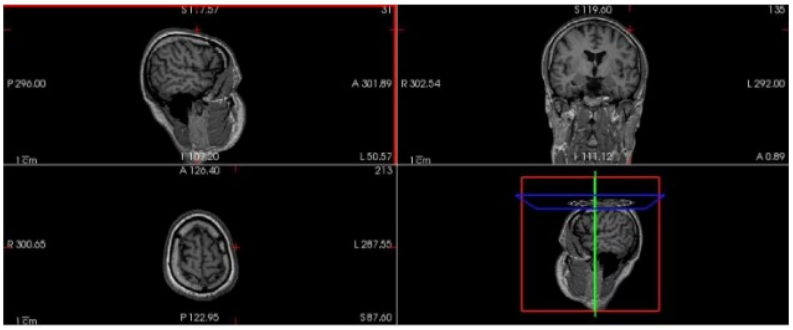

Fig 11. One of the two optimal coil placement locations for stimulation of fornix as indicated by the cross in top right and bottom left windows

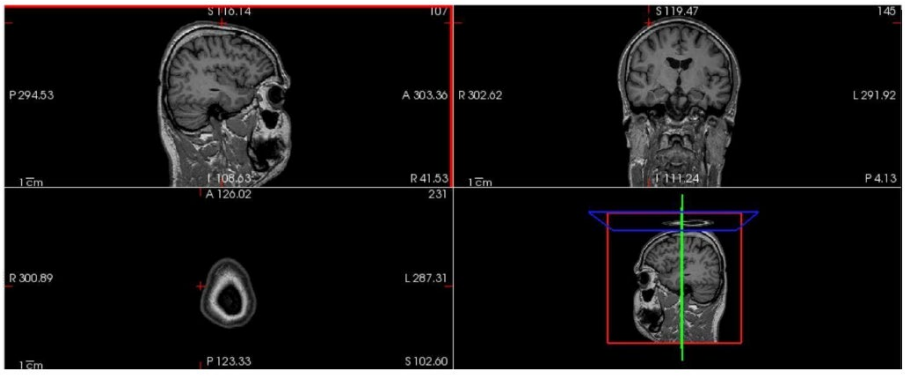

Fig 12. Second optimal coil placement location for stimulation of fornix as indicated by the cross in top right and bottom left windows

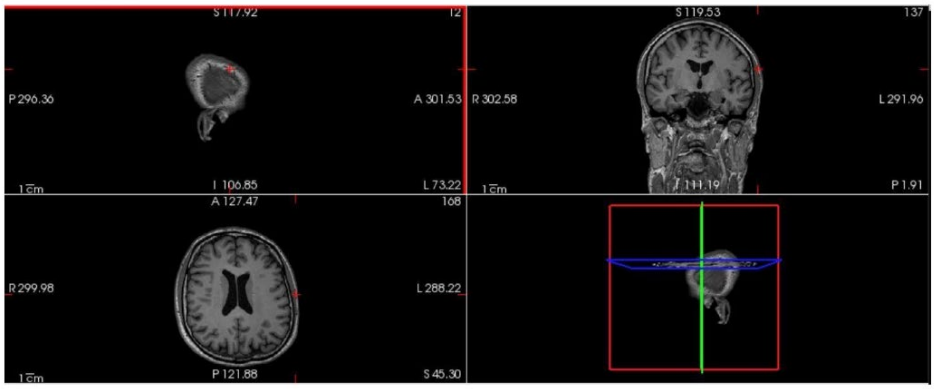

Fig 13. Optimal Coil Placement location for stimulation of veas indicated by the cross in top right and bottom left windows

Discussion

In this work, the use of TMS to target specific deeper brain structures commonly targeted by other stimulation techniques such as DBS was validated through magnetic field simulations as well as deriving optimal locations for coil placement to induce the desired magnetic fields. This work also supports the use of the H1-coil for stimulating deeper brain regions which was previously unclear. However, it was not possible to define any magnetic field intensity threshold for stimulation of these deeper brain structures at which stimulation is effective due to stimulation intensity requirements being variable between patients. Additionally, the intensity at which the coil emits magnetic waves can also be fine-tuned to match the patient's needs. Most optimal locations for stimulation were located on the left side of the brain, consistent with the traditional method of administering TMS to the left cerebral hemisphere due to the ability of the H1 coil being more effective in stimulating the left side rather than the right. Additionally, since there was only one cluster for all of the optimal coordinates corresponding to each brain structure excluding the fornix, the suggested optimal stimulatory locations were consistently validated.

Due to the presence of more than one optimal location for stimulation of the fornix, advanced simulations will be done in the future using the TMS Modelling Software Toolkit designed by researchers at the Massachusetts General Hospital in which multiple TMS coils can be used at the same time within one simulation. The presence of two optimal locations for fornix stimulation may have been caused by both locations producing similar magnetic fields from both sides of the brain that reach the target at similar intensities. This functionality can be used to assign two TMS coils, each corresponding to an optimal location for the fornix, and simulate with both coils simultaneously to investigate the effect of simultaneous stimulation. Other experimental techniques for stimulating with more than one coil will be tested including stimulating using an array of coils, along with different types of coils, stimulation intensities, and coil orientations.

Additionally, more advanced unsupervised learning techniques including variations of the K-means algorithm as well as gaussian mixture models will be used to analyze this data to reveal any further trends of interest.

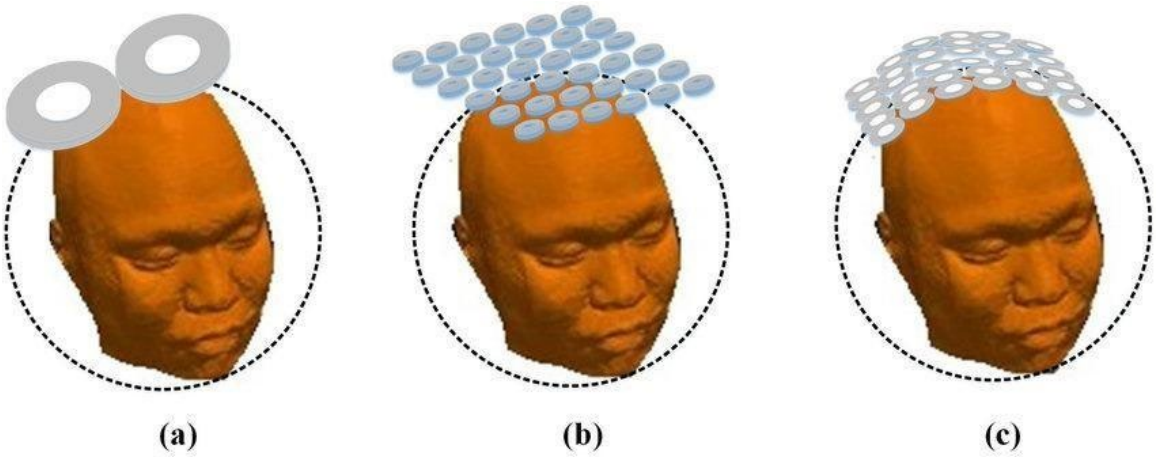

Figure 14. Multi-coil TMS arrays https:// www.researchgate.net/figure/Coil-arrays-used-for-comparison-a-Figure-8-coil-b-36-coil-planar-array-c-36-coil-fig3_321066255

Conclusion

This study demonstrates and validates the use of TMS for stimulation of deeper brain structures involved in neurological diseases and conditions. These optimal locations found for coil placement will help in guiding treatment for Parkinson's disease, epilepsy, PTSD, chronic pain, Alzheimer's disease, depression, and OCD which conventionally have not been treated using TMS. All structures consistently show one optimal site of coil placement excluding the fornix showing 2 optimal locations. This study has mathematically validated the stimulation of these brain structures, as a precedent to further work such as clinical trials. Further work done with these simulations may validate the use of deep TMS for other brain structures corresponding to other neurological conditions.

Acknowledgments

I would like to thank my advisor for the valuable insight provided to me on this topic.

References

Adolfo Ramirez-Zamora, M. D. (2018, March 1). *Pallidal or subthalamic nucleus deep brain stimulation for parkinson disease*. JAMA Neurology. Retrieved October 28, 2021, from https://jamanetwork.com/journals/jamaneurology/article-abstract/2670447.

authors, A., Tendler, A., & Additional informationFundingThis paper was funded by Brainsway Ltd. (n.d.). *Deep transcranial magnetic stimulation (dtms) – beyond depression.* Taylor & Francis. Retrieved October 28, 2021, from https://www.tandfonline.com/doi/full/10.1080/17434440.2016.1233812.

Børretzen, M. N., Bjerknes, S., Sæhle, T., Skjelland, M., Skogseid, I. M., Toft, M., & Dietrichs, E. (2014, June 5). *Long-term follow-up of thalamic deep brain stimulation for essential tremor – patient satisfaction and mortality*. BMC Neurology. Retrieved October 28, 2021, from

https://bmcneurol.biomedcentral.com/articles/10.1186/1471-2377-14-120.

Benabid AL;Krack PP;Benazzouz A;Limousin P;Koudsie A;Pollak P; (n.d.). *Deep brain stimulation of the subthalamic nucleus for parkinson's disease: Methodologic aspects and clinical criteria*. Neurology. Retrieved October 28, 2021, from https://pubmed.ncbi.nlm.nih.gov/11188974/.

Boccard, S. G. J., Prangnell, S. J., Pycroft, L., Cheeran, B., Moir, L., Pereira, E. A. C., Fitzgerald, J. J., Green, A. L., & Aziz, T. Z. (2017, July 11). *Long-term results of deep brain stimulation of the anterior cingulate cortex for neuropathic pain*. World Neurosurgery. Retrieved October 28, 2021, from https://www.sciencedirect.com/science/article/abs/pii/S1878875017310811.

Bove, F., Mulas, D., Cavallieri, F., Castrioto, A., Chabardès, S., Meoni, S., Schmitt, E., Bichon, A., Stasio, E. D., Kistner, A., Pélissier, P., Chevrier, E., Seigneuret, E., Krack, P., Fraix, V., & Moro, E. (2021, July 20). *Long-term outcomes (15 years) after subthalamic nucleus deep brain stimulation in patients with parkinson disease*. Neurology. Retrieved October 28, 2021, from https://n.neurology.org/content/97/3/e254.

D;, F. K. A. T.-R. (n.d.). *Deep brain stimulation of globus pallidus interna, subthalamic nucleus, and pedunculopontine nucleus for parkinson's disease: Which target?* Parkinsonism & related disorders. Retrieved October 28, 2021, from https://pubmed.ncbi.nlm.nih.gov/22166422/.

Daneshzand, M., Makarov, S. N., de Lara, L. I. N., Guerin, B., McNab, J., Rosen, B. R., Hämäläinen, M. S., Raij, T., & Nummenmaa, A. (2021, August 15). *Rapid computation of TMS-induced E-fields using a dipole-based magnetic stimulation profile approach*. NeuroImage. Retrieved October 28, 2021, from https://www.ncbi.nlm.nih.gov/pmc/articles/PMC8353625/.

Deng, Z.-D., Lisanby, S. H., & Peterchev, A. V. (2013, January). *Electric field depth-focality tradeoff in transcranial magnetic stimulation: Simulation comparison of 50 coil designs*. Brain stimulation. Retrieved October 28, 2021, from https://www.ncbi.nlm.nih.gov/pmc/articles/PMC3568257/.

Fricke, C., Duesmann, C., Woost, T. B., von Hofen-Hohloch, J., Rumpf, J.-J., Weise, D., & Classen, J. (1AD, January 1). *Dual-site transcranial magnetic stimulation for the treatment of parkinson's disease*. Frontiers. Retrieved October 28, 2021, from https://www.frontiersin.org/articles/10.3389/fneur.2019.00174/full.

Gomez, L. J., Dannhauer, M., & Peterchev, A. V. (2020, December 30). *Fast computational optimization of TMS coil placement for individualized electric field targeting*. NeuroImage. Retrieved October 28, 2021, from https://www.sciencedirect.com/science/article/pii/S1053811920311812?via%3Dihu b.

Greenberg, B. D., Gabriels, L. A., Malone, D. A., Rezai, A. R., Friehs, G. M., Okun, M. S., Shapira, N. A., Foote, K. D., Cosyns, P. R., Kubu, C. S., Malloy, P. F., Salloway, S. P., Giftakis, J. E., Rise, M. T., Machado, A. G., Baker, K. B., Stypulkowski, P. H., Goodman, W. K., Rasmussen, S. A., & Nuttin, B. J. (2008, May 20). *Deep brain stimulation of the ventral internal capsule/ventral striatum for obsessive-compulsive disorder: Worldwide experience*. Nature News. Retrieved October 28, 2021, from https://www.nature.com/articles/mp200855?error=cookies_not_supported&code=+bc085581-b166-4dd0-a994-4ab3ef7f3fc9.

Hamel, W., Fietzek, U., Morsnowski, A., Schrader, B., Herzog, J., Weinert, D., Pfister, G., Müller, D., Volkmann, J., Deuschl, G., & Mehdorn, H. M. (2003, August 1). *Deep brain stimulation of the subthalamic nucleus in parkinson's disease: Evaluation of active electrode contacts*. Journal of Neurology, Neurosurgery & Psychiatry. Retrieved October 28, 2021, from https://jnnp.bmj.com/content/74/8/1036.

Jin H;Li W;Dong C;Wu J;Zhao W;Zhao Z;Ma L;Ma F;Chen Y;Liu Q; (n.d.). *Hippocampal deep brain stimulation in nonlesional refractory Mesial Temporal Lobe epilepsy*. Seizure. Retrieved October 28, 2021, from https://pubmed.ncbi.nlm.nih.gov/26908151/.

Koek, R. J., Langevin, J.-P., Krahl, S. E., Kosoyan, H. J., Schwartz, H. N., Chen, J. W. Y., Melrose, R., Mandelkern, M. J., & Sultzer, D. (2014, September 10). *Deep brain stimulation of the basolateral amygdala for treatment-refractory combat post-traumatic stress disorder (PTSD): Study protocol for a pilot randomized controlled trial with blinded, staggered onset of stimulation*. Trials. Retrieved October 28, 2021, from https://www.ncbi.nlm.nih.gov/pmc/articles/PMC4168122/.

Kreuzer, P. M., Lehner, A., Schlee, W., Vielsmeier, V., Schecklmann, M., Poeppl, T. B., Landgrebe, M., Rupprecht, R., & Langguth, B. (2015, December 15). *Combined RTMS treatment targeting the anterior cingulate and the temporal cortex for the treatment of chronic tinnitus*. Nature News. Retrieved October 28, 2021, from https://www.nature.com/articles/srep18028?error=cookies_not_supported&code=+ +c3bb5eeb-f913-4820-96b1-ced614cc469c.

Leoutsakos JS;Yan H;Anderson WS;Asaad WF;Baltuch G;Burke A;Chakravarty MM;Drake KE;Foote KD;Fosdick L;Giacobbe P;Mari Z;McAndrews MP;Munro CA;Oh ES;Okun MS;Pendergrass JC;Ponce FA;Rosenberg PB;Sabbagh MN;Salloway S;Tang-Wai DF;Targum SD;Wolk D;Lozano AM;S. (n.d.). *Deep brain stimulation targeting the fornix for mild alzheimer dementia (the advance trial): A two year follow-up including results of delayed activation*. Journal of Alzheimer's disease : JAD. Retrieved October 28, 2021, from https://pubmed.ncbi.nlm.nih.gov/29914028/.

Lv, Q., Du, A., Wei, W., Li, Y., Liu, G., & Wang, X. P. (1AD, January 1). *Deep Brain Stimulation: A potential treatment for dementia in alzheimer's disease (AD) and parkinson's disease dementia (PDD)*. Frontiers. Retrieved October 28, 2021, from https://www.frontiersin.org/articles/10.3389/fnins.2018.00360/full.

Navarro de Lara, L. I., Daneshzand, M., Mascarenas, A., Paulson, D., Pratt, K., Okada, Y., Raij, T., Makarov, S. N., & Nummenmaa, A. (2021, January 1). *A 3-axis coil design for multichannel TMS arrays*. NeuroImage. Retrieved October 28, 2021, from https://www.ncbi.nlm.nih.gov/pmc/articles/PMC7837414/.

Nielsen, J. D., Madsen, K. H., Puonti, O., Siebner, H. R., Bauer, C., Madsen, C. G., Saturnino, G. B., & Thielscher, A. (2018, March 12). *Automatic skull segmentation from MR images for realistic volume conductor models of the head: Assessment of the state-of-the-art*. NeuroImage. Retrieved October 28, 2021, from https://www.sciencedirect.com/science/article/abs/pii/S1053811918301800?via%3 Dihub.

P;, P. M. B. G. Z. L. B. (n.d.). *Hippocampal deep brain stimulation: Persistent seizure control after bilateral extra-cranial electrode fracture*. Neurological sciences : official journal of the Italian Neurological Society and of the Italian Society of Clinical Neurophysiology.Retrieved October 28, 2021, from https://pubmed.ncbi.nlm.nih.gov/29756178/#:~:text=Hippocampal%20deep%20b rain%20stimulation%20(DBS,a%20bilateral%20hippocampal%20DBS%20devic e.

Russo, J. F., & Sheth, S. A. (2015, June 1). *Deep brain stimulation of the dorsal anterior cingulate cortex for the treatment of chronic neuropathic pain*. focus. Retrieved October 28, 2021, from https://thejns.org/focus/view/journals/neurosurg-focus/38/6/article-pE11.xml.

Samoudi, A. M., Tanghe, E., Martens, L., & Joseph, W. (2018, June 5). *Deep transcranial magnetic stimulation: Improved coil design and assessment of the induced fields using MIDA model*. BioMed Research International. Retrieved October 28, 2021, from https://www.hindawi.com/journals/bmri/2018/7061420/.

Schutter, D. J. L. G., & van Honk, J. (2005, March). *A framework for targeting alternative brain regions with repetitive transcranial magnetic stimulation in the treatment of depression*. Journal of psychiatry & neuroscience : JPN. Retrieved October 28, 2021, from https://www.ncbi.nlm.nih.gov/pmc/articles/PMC551160/.

Sims-Williams, H., Matthews, J. C., Talbot, P. S., Love-Jones, S., Brooks, J. C., Patel, N. K., & Pickering, A. E. (2017, February 1). *Deep brain stimulation of the periaqueductal gray releases endogenous opioids in humans*. NeuroImage. Retrieved October 28, 2021, from https://www.ncbi.nlm.nih.gov/pmc/articles/PMC5312788/#:~:text=Deep%20brain%20stimulation%20(DBS)%20of,positron%20emission%20tomography%20(PET).

Sturm, V., Fricke, O., Buehrle, C. P., Lenartz, D., Maarouf, M., Treuer, H., Mai, J. K., & Lehmkuhl, G. (1AD, January 1). *DBS in the basolateral amygdala improves symptoms of autism and related self-injurious behavior: A case report and hypothesis on the pathogenesis of the disorder*. Frontiers. Retrieved October 28, 2021, from https://www.frontiersin.org/articles/10.3389/fnhum.2012.00341/full.

Tanaka, R., Ansari, A., Kajita, Y., Yamada, Y., Kawase, T., & Kato, Y. (2019). *Staged deep brain stimulation of ventral intermediate nucleus of the thalamus for suppression of essential tremors*. Asian journal of neurosurgery. Retrieved October 28, 2021, from https://www.ncbi.nlm.nih.gov/pmc/articles/PMC6703004/.

Tao, Q., Yang, Y., Yu, H., Fan, L., Luan, S., Zhang, L., Zhao, H., Lv, L., Jiang, T., & Song, X. (2020, April 3). *Anatomical connectivity-based strategy for targeting transcranial magnetic stimulation as antidepressant therapy*. Frontiers in psychiatry. Retrieved October 28, 2021, from https://www.ncbi.nlm.nih.gov/pmc/articles/PMC7145890/.

Tendler, A., Roth, Y., Barnea-Ygael, N., & Zangen, A. (2017, January 23). *How to use the H1 deep transcranial magnetic stimulation coil for conditions other than depression*. Journal of visualized experiments : JoVE. Retrieved October 28, 2021, from https://www.ncbi.nlm.nih.gov/pmc/articles/PMC5352287/.

Theodore, W. H. (2003, November). *Transcranial magnetic stimulation in epilepsy*. Epilepsy currents. Retrieved October 28, 2021, from https://www.ncbi.nlm.nih.gov/pmc/articles/PMC321221/.

Weise, K., Numssen, O., Thielscher, A., Hartwigsen, G., & Knösche, T. R. (2019, December 23). *A novel approach to localize cortical TMS effects*. NeuroImage. Retrieved October 28, 2021, from https://www.sciencedirect.com/science/article/pii/S1053811919310778?via%3Dihu b.

Yazdanian, H., Saturnino, G. B., Thielscher, A., & Knudsen, K. (2020, March 19). *Fast evaluation of the BIOT-Savart integral using FFT for electrical conductivity imaging*. Journal of Computational Physics. Retrieved October 28, 2021, from https://www.sciencedirect.com/science/article/pii/S0021999120301820?via%3Dihu b.

Zhang, C., Li, D., Jin, H., Zeljic, K., & Sun, B. (2017, October). *Target-specific deep brain stimulation of the ventral capsule/ventral striatum for the treatment of neuropsychiatric disease*. Annals of translational medicine. Retrieved October 28, 2021, from https://www.ncbi.nlm.nih.gov/pmc/articles/PMC5673773/.

Zibman, S., Pell, G. S., Barnea-Ygael, N., Roth, Y., & Zangen, A. (2019, July 5). *Application of transcranial magnetic stimulation for major depression: Coil design and neuroanatomical variability considerations*. European Neuropsychopharmacology. Retrieved October 28, 2021, from https://www.sciencedirect.com/science/article/pii/S0924977X19302676.